ELSEVIER

Biochimica et Biophysica Acta 1373 (1998) 101–111

BIOCHIMICA ET BIOPHYSICA ACTA
BBA

Surface plasmon resonance analysis at a supported lipid monolayer

Matthew A. Cooper [a,*], Andrew C. Try [a], Joe Carroll [b], David J. Ellar [b], Dudley H. Williams [a]

[a] *Department of Chemistry, Cambridge Centre for Molecular Recognition, University of Cambridge, Lensfield Road, Cambridge CB2 1EW, UK*

[b] *Department of Biochemistry, Cambridge Centre for Molecular Recognition, University of Cambridge, Tennis Court Road, Cambridge CB2 1GA, UK*

Received 22 April 1998; accepted 20 May 1998

Abstract

Methods for the formation of supported lipid monolayers on top of a hydrophobic self assembled monolayer in a surface plasmon resonance instrument are described. Small unilamellar vesicles absorb spontaneously to the surface of the hydrophobic self-assembled monolayer to form a surface which resembles the surface of a cellular membrane. Lipophilic ligands, such as small acylated peptides or glycosylphosphatidylinositol-anchored proteins, were inserted into the absorbed lipid and binding of analytes to these ligands was analysed by surface plasmon resonance. Conditions for the formation of lipid monolayers have been optimised with respect to lipid type, chemical and buffer compatibility, ligand stability and reproducibility. © 1998 Elsevier Science B.V. All rights reserved.

Keywords: Surface plasmon resonance; Lipid monolayer; Kinetics; Glycopeptide antibiotic; Glycosylphosphatidylinositol; Aminopeptidase N; Cry1Ac; Toxin

1. Introduction

Many of the interactions studied in the biological and biomedical sciences occur at membrane surfaces. There are, however, very few methods that allow quantitative determination of such interactions. Most techniques for detailed analysis of molecular recognition events are applied in solution phase using a soluble form of the receptor. Membrane receptors typically possess hydrophobic domains and are likely to have different tertiary structures and binding affinities in solution relative to those occurring in a membrane environment. Therefore, the need exists for a technique that allows the analysis of membrane-associated receptor–analyte interactions in their native environment. Supported lipid monolayers can be formed on an alkane-thiol self-assembled monolayer, which is in turn mounted on a gold surface [1]. The lipid monolayer formed in this

Abbreviations: SPR, surface plasmon resonance; RU, response units; HPA chip, hydrophobic association sensor chip; CAPS, 3-[cyclohexylamino]-1-propanesulphonic acid; HBTU, 2-(1*H*-benzotriazole-1-yl)-1,1,3,3-tetramethylammonium hexafluorophosphate; SUV, small unilamellar vesicle; SDS, sodium dodecylsulphate; BSA, bovine serum albumin; APN, aminopeptidase N; GPI, glycosylphosphatidylinositol; PC, L-α-phosphatidylcholine; DMPC, dimyristoylphosphatidylcholine; DPPC, dipalmitoylphosphatidylcholine; DSPC, distearoylphosphatidylcholine; DAPC, diarachidonylphosphatidylcholine; POPC, palmitoyloleoylphosphatidylcholine; MIC, minimum inhibitory concentration; Gal-NAc, *N*-acetyl galactosamine

* Corresponding author. Fax: +44 (1223) 336913.
E-mail: mc221@cam.ac.uk

0005-2736/98/$19.00 © 1998 Elsevier Science B.V. All rights reserved.
PII: S0005-2736(98)00091-1

way provides a chemically and physically stable environment which resembles the surface of a cellular membrane, and the gold surface is suitable for surface plasmon resonance (SPR) analysis. Changes in the measured refractive index at the interface, given in response units, are proportional to the amount of material in the immediate vicinity of the sensor surface [2]. Buffered solutions of an analyte are passed over the surface and the affinity of the binding event can be calculated from analysis of the resultant binding curve.

Following the pioneering work of Vogel and coworkers [1], several applications exploiting this technology have been reported [3–5]. Whilst the analysis of receptor–analyte interactions in a membrane-like environment is now technically possible, there are no guidelines for experimental design published in the literature. This study redresses the relative paucity of information on the above model membrane system and demonstrates the utility of supported lipid monolayers in the analysis of two different membrane-associated interactions. A general methodology for formation of supported lipid monolayers containing lipophilic ligands is described and conditions have been optimised with respect to lipid type, chemical and buffer compatibility, ligand stability and reproducibility.

2. Materials and methods

Octyl D-glucoside, bovine serum albumin, L-α-phosphatidylcholine, dimyristoylphosphatidylcholine, dipalmitoylphosphatidylcholine, distearoylphosphatidylcholine and diarachidonylphosphatidylcholine were purchased from Sigma-Aldrich (UK). [^{3}H]dipalmitoylphosphatidylcholine was obtained from Amersham, UK. Disialylganglioside GD_{1a} was purchased from Matreya, (Pleasant Gap, PA). The isolation, purification and preparation of the insecticidal Cry toxin and its receptor, APN, has been described in detail elsewhere [6,7]. The synthesis of the acylated mucopeptide analogue *N*-α-docosanoyl-*N*-ε-acetyl-lysyl-D-alanyl-D-alanine used for the antibiotic binding experiments has been described previously [8]. The glycopeptide antibiotics biphenylchloroeremomycin (LY307599), chloroeremomycin (LY264826), eremomycin and vancomycin were a gift from Eli Lilly (Indianapolis, IN) Teicoplanin and teicoplanin aglycone A_3-1 were a gift from MMDR1 Lepetit Research Centre (Gerenzano, Italy). Ristocetin A was obtained from Abbot Laboratories (North Chicago, IL). The SPR instrument was a BIACORE 2000 (Biacore, UK) used with a hydrophobic association (HPA) chip which consisted of an octadecane-thiol self assembled monolayer on a gold surface. Each sensor chip contained four flow cells of dimensions $2.4\times0.5\times0.05$ mm ($l\times w\times h$) with a probing spot for the SPR signal of ca. 0.26 mm^2 for each flow cell.

2.1. Preparation of vesicles

2.1.1. Extrusion

Small unilamellar vesicles (SUV) were prepared [9] in phosphate buffer (100 mM Na_2HPO_4/NaH_2PO_4, pH 7.4) by extrusion. Typical procedure: egg yolk L-α-phosphatidylcholine (128 mg, 0.16 mmol) was dissolved in ethanol free chloroform (10 ml) in a 100 ml round bottom flask. The lipid was deposited as a thin film by removal of the solvent under reduced pressure on a rotary evaporator, then dried under high vacuum for 2 h. Phosphate buffer (8 ml) was then added to give a 20 mM suspension. The lipid was shaken for 30 min, sonicated in a bath sonicator for 2 min, then passed 17 times through a 50-nm polycarbonate filter in an Avestin Lipofast Basic extrusion apparatus to give a translucent solution.

2.1.2. Sonication

Vesicles were formed as a suspension in phosphate buffer as described above, then subjected to probe sonication in a MSE Soniprep 150 (3×10 min at 6 μm amplitude using a 3 mm microtip probe) and purified by ultracentrifugation [10].

2.2. Formation of lipid monolayers

The surface of an HPA sensor chip was cleaned by a 10 min injection of 40 mM octyl D-glucoside at a flow rate of 10 μl/min. The injection needle was cleaned by pre-dipping in water, then SUV (20 μl, 500 μM) injected immediately at a flow rate of 2 μl/min. The lipid layer was then washed at 100 μl/min with sodium hydroxide (10 mM, 20 μl). The degree of coverage of the surface was determined from the

amount of lipid bound at a stable level (after the sodium hydroxide wash) and from the extent of non-specific binding of BSA (0.1 mg/ml in phosphate buffer, 5 min injection). The usable lifetime of the sensor chip was assayed by repeated cycles of loading with egg PC SUV and cleaning with octyl D-glucoside as described above.

2.3. Measurement of lipid surface concentration

A mixture of [^{1}H]DPPC (2 mg in chloroform) and [^{3}H]DPPC (0.1 ml of a 110 μCi/ml solution in chloroform/toluene) was shaken at 50°C for 30 min, then deposited on the walls of a 100 ml round bottom flask by removal of solvent on a rotary evaporator. Small unilamellar vesicles were then formed in phosphate buffer by sonication, as described above. All four flow cells of a new HPA sensor chip were loaded with these vesicles (30 μl, 2 μl/min, 2 mM DPPC) at 40°C using phosphate buffer as the eluent, as described above. Following formation of a stable signal after loading with vesicles, octyl D-glucoside (75 μl, 15 μl/min, 40 mM) was injected across the surface and the elute collected for analysis. The process of loading with lipid and washing with detergent was repeated 20 times and all recovered fractions pooled. Octyl D-glucoside (1 ml, 40 mM) was added to the original [^{3}H]DPPC vesicle preparation (1 ml, 2 mM DPPC) to dissolve the lipid and then this sample and the pooled lipid-detergent fractions recovered from the sensor chip were diluted in Optiphase 'Hisafe 3' scintillation fluid (Fischer Scientific, UK) (10 ml). β-Radiation of the samples were measured using a TriCarb 2200 CA liquid scintillation analyser calibrated with an internal reference sample (Packard ^{3}H 253200 DPM). Scintillation counts were performed 10 times.

2.4. Preparation of t-Boc-D-γ-glutamyl(α-benzyl)-lysyl(N-ε-acetyl)-D-alanyl-D-alanine benzyl ester

t-Boc-*N*-ε-acetyl-lysyl-D-alanyl-D-alanine benzyl ester [8] (1.19 g, 2.29 mmol) was dissolved in dichloromethane (25 ml) and a solution of hydrochloric acid in dioxane (4 M, 8 ml) and the resulting mixture was allowed to stir for 2 h. The solvent was then removed and the last traces of hydrogen chloride were removed by the successive addition and evaporation of dichloromethane (3×20 ml). A solution of *t*-Boc-glutamic acid-α-benzyl ester (850 mg, 2.50 mmol), *N*,*N*-diisopropylethylamine (350 mg, 2.71 mmol) and HBTU (1.04 g, 2.74 mmol) in dichloromethane (20 ml) was stirred for 10 min and to this was added the crude *N*-ε-acetyl-lysyl-D-alanyl-D-alanine benzyl ester hydrochloride and *N*,*N*-diisopropylethylamine (820 mg, 6.34 mmol) in dichloromethane (30 ml). The resulting solution was stirred at room temperature for 4 h and the solvent removed. The residue obtained was chromatographed over silica (chloroform initially, then methanol/chloroform, 1:9) and the major band collected and evaporated to dryness to afford *t*-Boc-D-γ-glutamyl(α-benzyl)-lysyl(*N*-ε-acetyl)-D-alanyl-D-alanyl benzyl ester (1.54 g, 91%) as a white solid. ^{1}H-NMR (500 MHz; DMSO-d_6) δ 1.12–1.37 (19 H, m, 2×Ala CH_3, Boc CH_3, Lys δ and Lys γ), 1.40–1.50 (1 H, m, Lys β), 1.51–1.59 (1 H, m, Lys β), 1.69–1.77 (4 H, m, acetyl CH_3 and Glu β), 1.85–1.94 (1 H, m, Glu β), 2.10–2.27 (2 H, m, Glu γ), 2.95 (2 H, app q, Lys ε), 3.94–4.00 (1 H, m, Glu α), 4.11–4.18 (1 H, m, Lys α), 4.24–4.33 (2 H, m, 2×Ala α), 5.04–5.12 (4 H, m, 2×benzylic CH_2), 7.25 (1 H, d, *J* 7.6 Hz, Glu NH), 7.27–7.37 (10 H, m, aryl H), 7.68–7.76 (1 H, m, acetyl NH), 7.94 (1 H, d, *J* 7.4 Hz, Lys NH), 8.11 (1 H, d, *J* 7.8 Hz, Ala NH), 8.23 (1 H, d, *J* 6.9 Hz, Ala NH).

2.5. Preparation of N-docosanoyl-D-γ-glutamyl(α-benzyl)-lysyl(N-ε-acetyl)-D-alanyl-D-alanine benzyl ester

N-*t*-Boc-D-γ-glutamyl(α-benzyl)-lysyl(*N*-ε-acetyl)-D-alanyl-D-alanyl benzyl ester [8] (100 mg, 0.14 mmol) was dissolved in a mixture of dichloromethane (2 ml) and a solution of hydrochloric acid in dioxane (4 M, 4 ml) and stirred for 2 h. The solvent was then removed and the last traces of hydrogen chloride were removed by the successive addition and evaporation of dichloromethane (3×5 ml). A mixture of docosanoic acid (50 mg, 0.15 mmol), *N*,*N*-diisopropylethylamine (90 mg, 0.70 mmol) and HBTU (62 mg, 0.17 mmol) in dichloromethane (2 ml) and methanol (2 ml) was stirred for 10 min and to this was added the crude D-γ-glutamyl(α-benzyl)-lysyl(*N*-ε-acetyl)-D-alanyl-D-alanine benzyl ester hydrochloride and *N*,*N*-diisopropylethylamine (90 mg, 0.70 mmol) in dichloromethane (2 ml). The resulting sol-

ution was stirred at room temperature for 4 h and the solvent was removed. The residue obtained was then chromatographed over silica (chloroform initially, then methanol/chloroform, 2:98 through to 8:92). The major band was collected and evaporated to dryness to afford *N*-docosanoyl-D-γ-glutamyl(α-benzyl)-lysyl(*N*-ε-acetyl)-D-alanyl-D-alanine benzyl ester (85 mg, 87%) as a white solid. ^{1}H-NMR (500 MHz; DMSO-d_6) δ 0.83 (3 H, t, *J* 7.0 Hz, docos CH_3), 1.14 (3 H, d, *J* 7.1 Hz, Ala CH_3), 1.17–1.38 (43 H, m, 18×docos CH_2, Lys γ, Ala CH_3 and Lys δ), 1.40–1.51 (3 H, m, docos β and Lys β), 1.52–1.60 (1 H, m, Lys β), 1.71–1.82 (4 H, m, acetyl CH_3 and Glu β), 1.88–1.96 (1 H, m, Glu β), 2.08 (2 H, t, *J* 7.3 Hz, docos α), 2.13–2.21 (2 H, m, Glu γ), 2.96 (2 H, app q, Lys ε), 4.11–4.18 (1 H, m, Lys α), 4.20–4.31 (3 H, m, Glu α and 2×Ala α), 5.05–5.11 (4 H, m, 2×benzylic CH_2), 7.27–7.37 (10 H, m, aryl H), 7.69–7.74 (1 H, m, acetyl NH), 7.95 (1 H, d, *J* 7.5 Hz, Lys NH), 8.11 (1 H, d, *J* 7.9 Hz, Ala NH), 8.17 (1 H, d, *J* 7.4 Hz, Glu NH), 8.03 (1 H, d, *J* 7.0 Hz, Ala NH).

2.6. Preparation of *N*-docosanoyl-D-γ-glutamyl-lysyl(*N*-ε-acetyl)-D-alanyl-D-alanine (*N*-docosanoyl-EKAA)

N-docosanoyl-D-γ-glutamyl(α-benzyl)-lysyl(*N*-ε-acetyl)-D-alanyl-D-alanine benzyl ester [8] (80 mg, 0.08 mmol) was dissolved in a mixture of absolute ethanol (65 ml), dichloromethane (15 ml) and toluene (10 ml) and hydrogenated for 12 h at 1 atm over 5% palladium on charcoal (15 mg). The reaction mixture was then filtered through celite and evaporated to dryness to afford *N*-docosanoyl-D-γ-glutamyl-lysyl(*N*-ε-acetyl)-D-alanyl-D-alanine (57 mg, 87%) as a white solid. ^{1}H-NMR (500 MHz; DMSO-d_6) δ 0.84 (3 H, t, *J* 7.1 Hz, docos CH_3), 1.14–1.28 (44 H, m, 18×docosanyl CH_2, Lys γ and 2×Ala CH_3), 1.30–1.38 (2 H, m, Lys δ), 1.42–1.51 (3 H, m, docos β and Lys β), 1.52–1.62 (1 H, m, Lys β), 1.64–1.73 (1 H, m, Glu β), 1.75 (3 H, m, acetyl CH_3), 1.88–1.98 (1 H, m, Glu β), 2.09 (2 H, t, *J* 7.4 Hz, docos α), 2.16 (2 H, t, *J* 7.5 Hz, Glu γ), 2.96 (2 H, app q, Lys ε), 4.04–4.16 (3 H, m, Lys α, Glu α and Ala α), 4.23 (1 H, app quin, Ala α), 7.73–7.78 (1 H, m, acetyl NH), 7.92 (1 H, d, *J* 7.2 Hz, amide NH), 7.95 (1 H, d, *J* 7.4 Hz, amide NH), 8.02 (1 H, d, *J* 7.5 Hz, amide NH), 8.14 (1 H, d, *J* 7.2 Hz, Ala NH).

2.7. Deposition of ligands

Small acylated ligands (< 1000 Da) were inserted directly into a lipid monolayer by injection of dilute solutions (ca. 50 μM) across the monolayer at a flow rate of 10 μl/min. Larger molecules, such as the GPI anchored protein APN [11], did not associate at stable levels with a pre-formed lipid monolayer when injected across the surface as dilute solutions. Deposition of the GPI anchored protein APN was achieved by loading the sensor chip with protein-containing small unilamellar vesicles formed by shaking purified APN (100 nM) for 5 min with vesicles formed by extrusion of PC (500 μM) in phosphate buffer. The control surface (usually lipid alone) was always in the first flow cell of the SPR instrument to prevent contamination from other flow cells containing ligand.

2.8. Stability of the lipid monolayer

Lipid monolayers formed as described above were exposed to a number of reagents that disrupt ligand–ligate complexes. The following reagents were injected across the surface for 2 min at a flow rate of 20 μl/min: 10% ethanol/water, 10% dimethylsulphoxide/water, 10% ethanolamine/water, 2 M sodium chloride, 2 M potassium chloride, 10 mM glycine (pH 2), 10 mM sodium carbonate, 100 mM cysteine hydrochloride and 100 mM hydrochloric acid. The stability of the lipid layer following exposure to the above reagents was assayed by flowing phosphate buffer at a rate of 10 μl/min across the surface for 18 h.

2.9. Cry1Ac purification and activation

Bacillus thuringiensis subsp. *kurstaki* HD73 expressing the Cry1Ac toxin was grown as described for *Bacillus megaterium* KM [12]. The Cry1Ac crystal inclusions were purified from sporulated *B. thuringiensis* cultures using discontinuous sucrose gradients [6] and the protein concentration was determined by the method of Lowry et al. [13] using BSA as a standard. Solubilisation of the Cry1Ac crystal in 50 mM Na_2CO_3/HCl, pH 9.5, plus 10 mM DTT, activation with *Pieris brassicae* gut extract and SDS-PAGE analysis were carried out as described previously [6].

2.10. Cry toxin binding assay

Activated Cry1Ac toxin was separated from small molecular mass digest products using a Micro Bio-spin 30 chromatography column (Bio-Rad) following the manufacturer's instructions. This step also exchanged the toxin incubation buffer with CAPS buffered saline (10 mM CAPS, KOH, 150 mM NaCl, pH 10). Quantification of the activated toxin preparations was carried out from UV absorbance at 280 nm and corrected using control enzyme preparations. Toxin was diluted in CAPS buffered saline from 500 to 16 nM and was passed serially at a flow rate of 20 μl/min over a flow cell containing lipid alone, then over a flow cell containing lipid and APN receptor. The sample solution was then replaced by buffer and the toxin–receptor complex allowed to dissociate for 4 min. The stability of the toxin–receptor complex was then assayed by 20 μl injections of 10 mM NaOH, 10 mM HCl, 1 M KCl and 100 mM GalNAc. All assays were carried out at 25°C. Data were prepared for analysis by subtracting the average response recorded 20 s prior to injection and adjusting the time of each injection to zero. Data from the flow cell containing lipid alone was then subtracted from corresponding data obtained from the receptor-containing flow cell to correct for bulk refractive index changes. Analysis was carried out using BIAevaluation 3.0 global analysis software based on algorithms for numerical integration [14].

2.11. Antibiotic binding assay

Glycopeptide antibiotics were diluted serially in phosphate buffer (100 mM, pH 7.4) from 4 to 0.63 μM and were passed sequentially over a control flow cell containing a lipid monolayer alone, then over a flow cell containing lipid and 200 response units (RU) of *N*-docosanoyl-L-Lys(Ac)-D-Ala-D-Ala [8] at a flow rate of 20 μl/min. The sample solution was then replaced by phosphate buffer and the analyte–receptor complex allowed to dissociate. Regeneration of the free ligand was effected by a 1 min injection of 10 mM hydrochloric acid. Five dummy runs of binding and regeneration were performed before data acquisition. All assays were carried out at 25°C. Data were prepared and analysed as described above for the toxin binding assay.

2.12. Data analysis

Analysis was carried out by non-linear fitting of data corrected for bulk refractive index changes as described above using BIAeval 3.0 global analysis software based on algorithms for numerical integration [14,15].

For the simple bimolecular association, $A+B=AB$, the process was assumed to be pseudo first order with no interaction between separate receptor molecules. The dissociation rate is derived from the equation:

$$R_t = R_{t_0} e^{-k_d(t-t_0)} \quad (1)$$

where R_t is the response at time t, R_{t_0} is the response at time t_0 and k_d is the dissociation rate constant. The association rate constant can be derived using the equation:

$$R_t = \frac{k_a C R_{max}(1-e^{-(k_a C+k_d)t})}{k_a C + k_d} \quad (2)$$

where R_{max} is the maximum response (proportional to the amount of immobilised ligand), C is the concentration of analyte in solution, and k_a is the association rate constant.

Affinities were calculated from the ratio of k_a/k_d and also from analysis of equilibrium binding levels at varying analyte concentration. By measuring the resonance units attained at equilibrium as a function of analyte concentration, affinities can be determined from a Scatchard analysis using the equation:

$$\frac{R_{eq}}{C} = K_a R_{max} - K_a R_{eq} \quad (3)$$

where R_{eq} is the response at equilibrium and K_a is the association constant. A plot of R_{eq}/C versus C has a slope of $-K_a$.

3. Results and discussion

3.1. Formation of lipid monolayers

Lipid monolayers were formed on the HPA chip using small unilamellar vesicles prepared from phosphatidylcholine (PC) by probe sonication, and also by extrusion. The propensity for the different vesicle preparations to form stable monolayers on the sen-

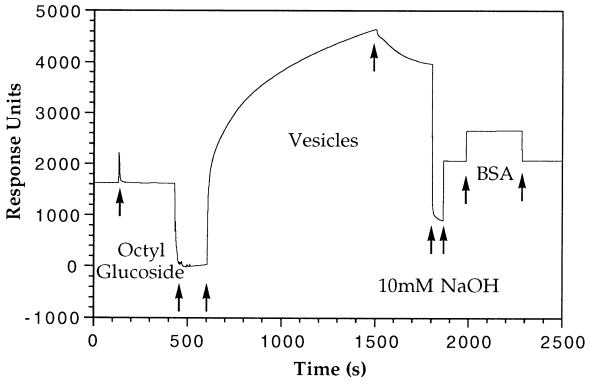

Fig. 1. Formation of a lipid monolayer with small unilamellar phosphatidylcholine vesicles. Formation of a stable lipid monolayer by successive injections of octyl-D-glucoside (40 mM), small unilamellar phosphatidylcholine vesicles (50 nm, 500 μM), sodium hydroxide (10 mM), then BSA (0.1 mg/ml) over an HPA sensor chip using phosphate buffer as eluent. Arrows indicate the beginning and end of each injection.

sor chip was assayed by examining the amount of lipid deposited, and the extent of non-specific binding of BSA, which binds significantly to the sensor chip in the absence of lipid (data not shown). Optimal coverage of the sensor chip in all cases was obtained when vesicles were injected over the surface at low flow rate immediately following a cleansing pulse of octyl D-glucoside. This resulted in an unstable signal ca. 4000 RU above the original level, possibly due to multilamellar structures on the sensor chip. Washing the surface with base resulted in a stable signal of ca. 2200 RU (Fig. 1). There was little difference in the degree of coverage of the sensor chip between vesicles formed by sonication or by extrusion and between injections of a low concentration of vesicles over several hours or a single injection at higher concentration (Table 1).

The SPR response was correlated with surface concentration on the HPA sensor chip using ^{3}H-labelled dipalmitoylphosphatidylcholine ([^{3}H]DPPC). Vesicles containing [^{3}H]DPPC were loaded onto a sensor chip and the lipid layer was then washed off with detergent. Scintillation counts of lipid-containing fractions recovered from the sensor chip showed good reproducibility with a relative standard deviation of less than 0.5%. Comparison of the average scintillation count in the recovered fractions with that obtained for the [^{3}H]DPPC vesicle preparation used to form the lipid layers enabled determination of the total amount of lipid absorbed on the sensor chip. The correlation with response units was 0.92 ± 0.05 pg mm^{-2} RU^{-1}, an identical value to that reported [2] for absorption of ^{35}S- and ^{14}C-labelled proteins onto a dextran hydrogel-derivatised CM5 sensor chip. 2200 RU of PC loaded on an HPA chip of area 1.2 mm^{2} thus corresponds to a surface lipid density of 2.0 ng mm^{-2} or 2.6 pmol mm^{-2}, and an area per lipid molecule of 64 Å^{2}. The calculated surface density is approximately half that reported [16] for a supported lipid bilayer (5.5 pmol mm^{-2}) and the calculated lipid head group area agrees well with the value determined [17] for hydrated DPPC by continuous X-ray scattering (66 Å^{2}). The surface capacity of the HPA sensor chip is lower than that of the CM5 chip (50 ng mm^{-2}) as the HPA surface is planar, whereas the CM5 surface is coated with a ca. 200 nm thick hydrogel [2].

The degree of non-specific binding of BSA to the sensor chip increased upon repeated cycles of loading with lipid and cleaning with detergent (Fig. 2). For the first 10 cycles of loading and cleaning, the amount of lipid bound to the surface decreased, but the surface remained biospecific. After ten cycles, a dramatic jump in the amount of non-specific binding of BSA occurred. There was significant variation

Table 1
Formation of lipid monolayers on an HPA sensor chip with small unilamellar phosphatidylcholine vesicles formed by extrusion, and by sonication

SUV injected (no. of injections × concentration)	Initial loading[a]	Loading after NaOH wash[a]	BSA bound[a,b]
Extruded 1 × 500 μM	4600 (240)	2390 (190)	30 (4)
Extruded 5 × 100 μM	4880 (210)	2430 (120)	0 (0)
Sonicated 1 × 500 μM	2740 (170)	2010 (100)	40 (7)
Sonicated 5 × 100 μM	3770 (190)	2350 (170)	10 (2)

[a]Values given as response units with standard deviations in brackets for $n = 3$.
[b]Ubiquitin gave nearly identical values to BSA.

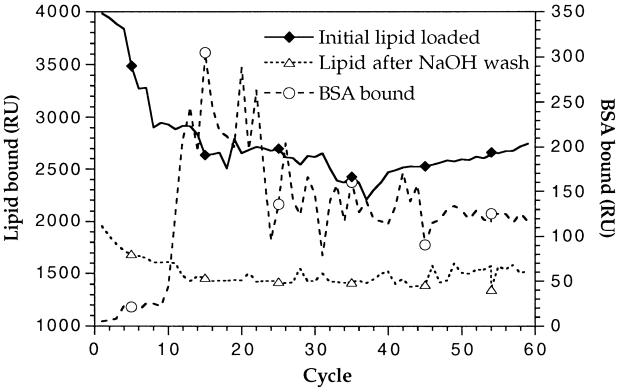

Fig. 2. Repeated loading of an HPA sensor chip with phosphatidylcholine vesicles. Amount of lipid initially bound (♦), bound after sodium hydroxide wash (△), and amount of BSA bound (○), to an HPA sensor chip upon repeated loading of phosphatidylcholine small unilamellar vesicles as described in Section 2.

in the usable lifetime of sensor chips from different manufactured batches. Attempts to regenerate the surface of an effete sensor chip with Triton X-100 or sodium dodecylsulphate (SDS) were unsuccessful.

Vesicles were successfully loaded onto the sensor chip in a number of common biological buffers, but not in low ionic strength buffer (Table 2). Comparison of lipid loaded in 10 mM Tris-EDTA (TE) and 100 mM NaCl-Tris-EDTA (STE) shows that the coverage of the sensor chip with lipid, as indicated by the amount of non-specific binding of BSA, was much less for TE than for STE (Table 2). PC monolayers were stable with many reagents (described in Section 2) used for regeneration of free ligand from bound analyte. The amount of lipid deposited on the surface of the sensor chip was stable following exposure to these reagents, as the response level did not change more than the level of intrinsic drift of the instrument (±0.3 RU/min).

3.2. Ligand stability and lipid type

Stable immobilised ligand levels are of paramount importance for SPR analysis. This is especially pertinent when using the HPA sensor chip, as the immobilised ligand is not covalently attached to the surface, but held in place by hydrophobic interactions. It should be noted that prevention of dissociation of the ligand from the monolayer is of primary importance for experimental design, because if the dissociation rate of the analyte–ligand complex is comparable to the dissociation rate of the ligand from the lipid monolayer, spurious results will be obtained. It was found that acylated small molecules were best deposited on the chip by injection as dilute solutions over a pre-formed lipid monolayer. The amount of ligand inserted, measured in response units (RU), was directly proportional to the injection time, up to a level of ca. 2000 RU (data not shown). Membrane-associated proteins were best deposited on the chip together with lipid from protein-containing small unilamellar vesicles which were formed by extrusion.

A number of amphipathic molecules were assayed for their affinity for a PC lipid monolayer. The mucopeptide bacterial cell wall analogue *N*-α-decanoyl-

Table 2
Loading of an HPA sensor chip with PC SUV (50 nm, 500 μM) in different buffers

Buffer	pH of buffer	Initial loading[g]	Loading after NaOH wash[g]	BSA bound[g]
Phosphate[a]	7.4	4600 (240)	2390 (190)	30 (4)
Citrate[b]	5.0	11100 (1100)	2120 (210)	20 (6)
10 mM TE[c]	8.0	1960 (160)	1780 (140)	900 (110)
100 mM STE[d]	8.0	4560 (250)	2060 (120)	10 (4)
HEPES[e]	8.0	4610 (270)	2100 (140)	70 (5)
CAPS[f]	10.0	2200 (180)	2020 (160)	60 (5)

[a]100 mM Na_2HPO_4/NaH_2PO_4.
[b]100 mM sodium citrate/NaH_2PO_4.
[c]Tris-HCl 10 mM, EDTA 1 mM.
[d]Tris-HCl 10 mM, EDTA 1 mM, NaCl 100 mM.
[e]10 mM *N*-(2-hydroxyethyl) 1-piperazine-*N*′-(2-ethanesulphonic acid), 100 mM NaCl.
[f]10 mM 3-cyclohexylamino-1-propane sulphonate, 150 mM NaCl.
[g]Values given as response units with standard deviations for $n=3$.

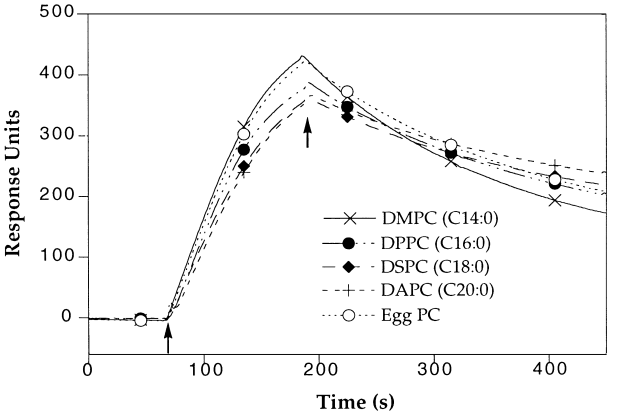

Fig. 3. Injection of the amphipathic peptide *N*-docosanoyl-EKAA across lipid monolayers composed of different types of lipid. Lipid monolayers were formed in phosphate buffer as described in Section 2 from small unilamellar vesicles composed of DMPC (×), DPPC (●), DSPC (♦), DAPC (+) and PC (○). Their ability to anchor the amphipathic peptide *N*-docosanoyl-EKAA was then assayed by injections of the peptide (30 μl, 20 μM) at a flow rate of 10 μl/min across the different monolayers.

L-Lys(Ac)-D-Ala-D-Ala, which possesses a C_{10} lipophilic anchor, showed relatively low affinity for a PC monolayer ($K_a = 4.3 \times 10^3$ M^{-1}). This value is comparable with the value ($K_a = 3.4 \times 10^3$ M^{-1}) calculated for the association of a similar peptide (*N*-α-decanoyl-Gly-Ala-Ala) with PC vesicles, determined by electrophoretic mobility and equilibrium dialysis measurements [18]. Peptides with a hydrophobic anchor possessing low affinity for the lipid layer may not, therefore, remain immobilised in the lipid upon binding to an analyte where the effect of the analyte is to increase the aqueous solubility of the peptide. *N*-Docosanoyl-L-Lys(Ac)-D-Ala-D-Ala, which possesses a C_{22} lipophilic anchor, showed a much higher affinity for the monolayer ($K_a = 8.3 \times 10^6$ M^{-1}) and was used in subsequent glycopeptide antibiotic binding experiments. The disialyganglioside, GD_{1a}, bound to lipid with a very high affinity ($K_a = 7 \times 10^9$ M^{-1}), with a dissociation rate constant below the limits of detection of the SPR instrument (i.e. $k_d < 10^{-5}$ s^{-1}). Aminopeptidase N (APN) [11] a glycosylphosphatidylinositol-anchored protein also possessed a high affinity ($K_a = 1.9 \times 10^8$ M^{-1}) for the PC monolayer.

The amphipathic peptide *N*-docosanoyl-D-γ-Glu-L-Lys(Ac)-D-Ala-D-Ala *N*-docosanoyl-EKAA was used as a probe to determine the efficacy of different lipid types to anchor small ligands with hydrophobic tails. Lipid monolayers were formed from lipids with varying acyl chain length and possessing different transition temperatures from the gel-like to the liquid crystal-like state [19]. The results show that binding of *N*-docosanoyl-EKAA to these lipid monolayers did not vary significantly between different lipid types (Fig. 3). Lipid monolayers were best formed when the lipid was used above its phase transition temperature and in a liquid crystal-like state. At 25°C, egg yolk PC, DMPC and unsaturated lipids, such as POPC, should result in a fluid monolayer [19].

3.3. Toxin binding to a GPI anchored membrane receptor

Post-translationally added glycoinositol phospholipids serve as membrane anchors for a wide variety of outer membrane proteins. By substituting the 3′-mRNA end sequence which codes for naturally occurring GPI-anchored proteins (i.e. that sequence which directs GPI anchoring) for endogenous 3′-mRNA, virtually any protein can be expressed as a GPI anchored derivative [20]. Aminopeptidase N (APN) is a well characterised GPI anchored protein that acts as a receptor for the δ-endotoxin Cry1Ac, a bacterial toxin isolated from *B. thuringiensis* which possesses potent insecticidal activity [7,11]. The toxin is initially translated as an inactive protoxin which is cleaved and activated by proteases in the midgut of the insect. It is thought to undergo a conformational change upon binding to APN which results in toxin pore formation in the epithelial cell membrane of the insect midgut [21].

Purified APN receptor was deposited on the sensor chip together with lipid using extruded PC vesicles shaken in an aqueous suspension of the receptor. Binding studies were carried out in CAPS buffered saline at pH 10.0, conditions approximating the alkaline conditions in the target lepidopteran insect gut [21]. At least some of the receptor appeared to be correctly inserted on the surface of the monolayer as specific binding of activated Cry1Ac to the APN-lipid monolayer compared to the lipid monolayer alone was observed (Fig. 4). Cry1Ac bound to the receptor in a biphasic manner; the initial association was very fast ($t = 0$–10 s), followed by a slower step

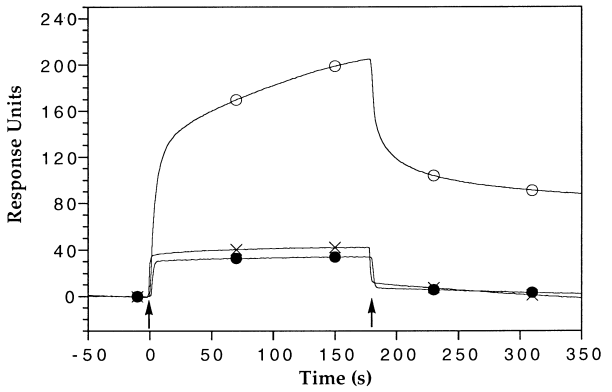

Fig. 4. Binding of Cry1Ac toxin and proteases to an APN-lipid monolayer. Injections of activated Cry1Ac toxin at 125 nM (○) and gut extract proteases control (×) over an APN-lipid monolayer. There was no binding of proteases used to activate the toxin. There was no binding of activated Cry1Ac toxin to the control surface composed of lipid alone (●). The data for binding of Cry1Ac to the APN-lipid monolayer has been corrected for bulk refractive index changes by subtraction of data for binding to the control surface consisting of lipid alone. No such correction has been made to the controls.

(t = 20–180 s) (Fig. 4). After an initial fast dissociation, the SPR signal did not return to original baseline levels, but remained stable at a higher level. Toxin thus associated with the monolayer could not be removed with reagents (described in Section 2) that normally disrupt weak interactions, or by 100 mM *N*-acetylgalactosamine, which has been shown to completely inhibit binding of the toxin to the receptor upon pre-incubation with toxin [22]. It is highly likely that in the stable complex, the toxin is embedded in the lipid monolayer and hence resistant to dissociation by reagents in the aqueous phase. The toxin thus appears to bind rapidly to the receptor, then there is a slow step which is believed to be associated with insertion of the toxin into the lipid monolayer.

The calculated affinity of the toxin for the APN-lipid monolayer was 3.0 nM, which approaches the affinity range, 0.2–1.6 nM, previously reported for radiolabelled Cry1Ac toxin interactions with receptor containing vesicles [23,24]. An affinity of 95 nM was reported [22] for the Cry1Ac interaction with solubilised APN immobilised on a dextran matrix sensor chip in the absence of other membrane components. This is much lower than the affinity range noted above for the radiolabelled binding studies and suggests that this value is only a measure of the initial binding event.

3.4. Glycopeptide antibiotic binding to bacterial mucopeptide analogues

The emergence of vancomycin-resistant enterococci (VRE) and the accompanying increase in the number of deaths from bacterial infections has given new urgency to studies of the clinically important glycopeptide antibiotics. We have shown previously that glycopeptide antibiotics dimerise in aqueous solution [25] and that antibiotics with high dimerisation constants are generally potent inhibitors of bacterial growth [26]. We have proposed that the glycopeptide antibiotics are able to bind co-operatively as dimers

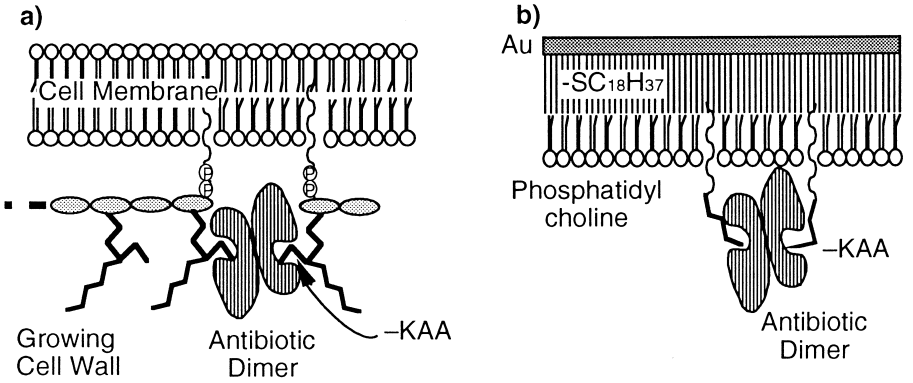

Fig. 5. Supported lipid monolayer model of glycopeptide antibiotic binding. (a) Disruption of peptidoglycan synthesis by binding of an antibiotic dimer to nascent mucopeptide terminating in the sequence L-Lys-D-Ala-D-Ala. (b) Supported lipid monolayer model of a bacterial membrane with antibiotic dimer binding to lipoylated peptide terminating in the sequence L-Lys-D-Ala-D-Ala.

to two nascent mucopeptides at the bacterial membrane surface, thereby disrupting cell wall synthesis (Fig. 5a). The target mucopeptide precursors terminate in the sequence L-Lys-D-Ala-D-Ala [27]. Peptides of varying length terminating in this sequence have been linked via their N-termini to a lipophilic anchor [8] for insertion in a supported lipid monolayer. This has allowed analysis of glycopeptide antibiotic activity at a model membrane surface (Fig. 5b).

The glycopeptide antibiotic chloroeremomycin bound to the amphipathic mucopeptide analogue *N*-docosanoyl-L-Lys(Ac)-D-Ala-D-Ala to reproducible response levels for up to 40 cycles of binding and regeneration (Fig. 6). The observed association rate of the antibiotics did not vary significantly when the flow rate was increased from 20 to 80 μl/min indicating the interaction was not mass transport limited [28].

Affinity constants of antibiotics for the mucopeptide analogue, calculated by Scatchard analysis of the steady state response attained at varying concentration, showed a correlation with observed antimicrobial activity in vitro (Fig. 7). In contrast, binding affinities calculated [26] for antibiotics with peptide in free solution showed no correlation with antimicrobial activity [4]. The affinities of the strongly dimerising antibiotics for peptide anchored in the lipid monolayer are higher than those for peptide measured in free solution. In conjunction with other evidence [26,29] this result suggests that at the surface the antibiotic dimer can bind co-operatively to two peptides (Fig. 5b). Those antibiotics with high dimerisation constants and those possessing lipophilic membrane anchors showed the highest affinity for peptide [4]. These two locating devices are thought to be crucial for activity against VRE [30].

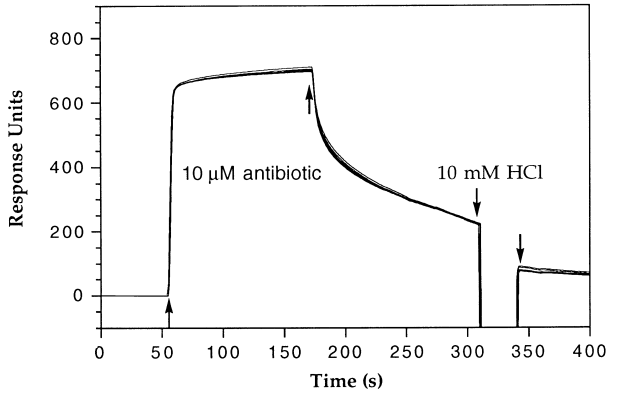

Fig. 6. Repeated binding of chloroeremomycin to a *N*-docosanoyl-KAA/lipid monolayer. Forty successive injections of the glycopeptide antibiotic chloroeremomycin (60 μl, 10 μM) at a flow rate of 20 μl/min to a *N*-docosanoyl-KAA/lipid monolayer, followed by regeneration of the surface with hydrochloric acid (10 μl, 10 mM). (Traces superimposed and every fifth cycle of binding and regeneration shown for clarity.)

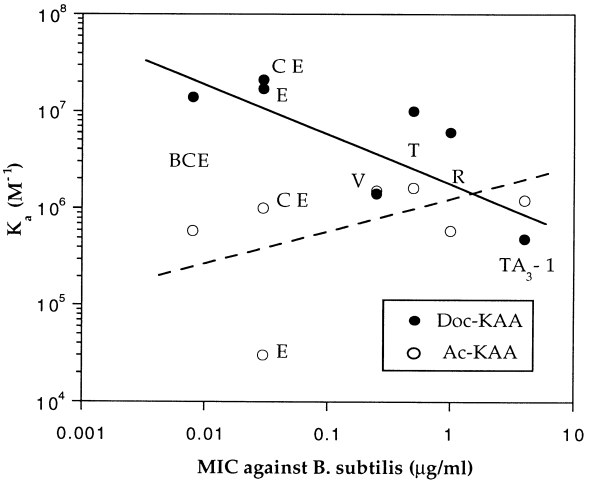

Fig. 7. Correlation between surface/solution binding constants of glycopeptide antibiotics to mucopeptide analogues and MICs. Correlation between MIC values against *Bacillus subtilis* and surface affinity constants of glycopeptide antibiotics to the lipid anchored mucopeptide analogue *N*-docosanoyl-KAA (●). Solution affinity constants [26] to the non-anchored analogue *N*-acetyl-KAA (○) do not correlate with MIC values. BCE, biphenylchloroeremomycin (LY307599); CE, chloroeremomycin (LY264826); E, eremomycin; V, vancomycin; T, teicoplanin; R, ristocetin A; TA_3-1, teicoplanin aglycone A_3-1.

4. Conclusions

The HPA sensor chip employed in an SPR instrument enables kinetic analysis of interactions at a model membrane surface. The methodology described in this paper possesses some advantages over methodologies using dextran matrix-based sensor chips as the lipid monolayer is a more biospecific surface than the negatively charged dextran matrix. Receptors in a lipid monolayer are mobile in the plane of the lipid [31] and thus the model system is well suited for the analysis of dimerising and co-operative interactions.

Acknowledgements

We thank the EPSRC (M.A.C.), Xenova (A.C.T.), BBSRC (D.J.E. and J.C.) and CCMR for financial support and Sanj Kumar of Biacore AB, UK for providing initial access to a demonstration BIACORE 2000 instrument.

References

[1] S. Terrettaz, T. Stora, C. Duschl, H. Vogel, Langmuir 9 (1993) 1361–1369.
[2] E. Stenberg, B. Persson, H. Roos, C. Urbaniczky, J. Colloid Interface Sci. 143 (1991) 513–526.
[3] G.M. Kuziemko, M. Stroh, R.C. Stevens, Biochemistry 35 (1996) 6375–6384.
[4] M.A. Cooper, D.H. Williams, Y.R. Cho, J. Chem. Soc. Chem. Commun. (1997) 1625–1626.
[5] A.L. Plant, M. Burke, E.C. Petrella, D.J. O'Shannessy, Anal. Biochem. 226 (1995) 342–348.
[6] J. Carroll, D.J. Ellar, Eur. J. Biochem. 214 (1993) 771–778.
[7] P.J. Knight, N. Crickmore, D.J. Ellar, Mol. Microbiol. 11 (1994) 429–436.
[8] A.C. Try, G.J. Sharman, R.J. Dancer, B. Bardsley, R.M.H. Entress, D.H. Williams, J. Chem. Soc. Perkin Trans. 1 (1997) 2911–2919.
[9] R.C. MacDonald, R.I. MacDonald, B.M. Menco, K. Takeshita, N.K. Subbarao, L. Hu, Biochim. Biophys. Acta 1061 (1991) 297–303.
[10] J. Storch, A.M. Kleinfel, Biochemistry 25 (1986) 1717–1726.
[11] P.J.K. Knight, B.H. Knowles, D.J. Ellar, J. Biol. Chem. 270 (1995) 17765–17770.
[12] G.S.A.B. Stewart, K. Johnstone, E. Hagelberg, D.J. Ellar, Biochem. J. 198 (1981) 101–106.
[13] O.H. Lowry, N.J. Rosebrough, A.L. Farr, R.J. Randall, J. Biol. Chem. 193 (1951) 265–275.
[14] R.L. Burden, J.D. Faires, Numerical Analysis, 5th edn., PWS-Kent Publishing Compay, Boston, 1993.
[15] D.J. O'Shannessy, M. Brigham-Burke, K.K. Soneson, P. Hensley, Anal. Biochem. 212 (1993) 457.
[16] P. Nollert, H. Kiefer, F. Jahnig, Biophys. J. 69 (1995) 1447–1455.
[17] B.A. Lewis, D.M. Engelman, J. Mol. Biol. 166 (1983) 211–217.
[18] R.M. Peitzsch, S. McLaughlin, Biochemistry 32 (1993) 10436–10443.
[19] A. Blume, Biochemistry 22 (1983) 5436–5442.
[20] M.E. Medof, S. Nagarajan, M.L. Tykocinski, FASEB J. 10 (1996) 574–586.
[21] B.H. Knowles, Adv. Insect. Physiol. 24 (1994) 275–308.
[22] L. Masson, Y. Lu, A. Mazza, R. Brousseau, M.J. Adang, J. Biol. Chem. 270 (1995) 20309–20315.
[23] S.F. Garczynski, J.W. Crim, M.J. Adang, Appl. Environ. Microbiol. 57 (1991) 2816–2820.
[24] J. Van Rie, S. Jansens, H. Höfte, D. Degheele, H.V. Mellaert, Eur. J. Biochem. 186 (1989) 239–247.
[25] J.P. Mackay, U. Gerhard, D.A. Beauregard, M.S. Westwell, M.S. Searle, D.H. Williams, J. Am. Chem. Soc. 116 (1994) 4581–4590.
[26] D.A. Beauregard, D.H. Williams, M.N. Gwynn, D.J.C. Knowles, Antimicrob. Agents Chemother. 39 (1995) 781–785.
[27] J.C.J. Barna, D.H. Williams, M.L. Williamson, J. Chem. Soc. Chem. Commun. (1985) 254–256.
[28] D.G. Myszka, T.A. Morton, M.L. Doyle, I.M. Chaiken, Biophys. Chem. 64 (1997) 127–137.
[29] M.S. Westwell, B. Bardsley, A.C. Try, R.J. Dancer, D.H. Williams, J. Chem. Soc. Chem. Commun. (1996) 589–590.
[30] G.J. Sharman, A.C. Try, R.J. Dancer, Y.R. Cho, T. Staroske, B. Bardsley, A.J. Maguire, M.A. Cooper, D.P. O'Brien, D.H. Williams, J. Am. Chem. Soc. 119 (1997) 12041–12047.
[31] D. Beyer, G. Elender, W. Knoll, M. Kuhner, S. Maus, H. Ringsdorf, E. Sackmann, Angew. Chem. 35 (1996) 1682–1685.